

Chapter 2

Experimental Development

2.1 Reaction System

In order to perform photocatalytic tests on compounds, a suitable reactor was fabricated based on previous successful designs in the literature [1–4]. The photocatalytic water splitting reaction is normally monitored by recording amount of product formed in a relatively small fixed volume batch reactor, over a set period of time. Therefore it is suitable to use a simple gas tight batch reactor for lab based testing, with an optical window for illumination. Most reactors used in the field can either be externally illuminated by a light source from the top down, or using a horizontal window (internal illumination is not considered). In this study, a side window will be used, as the choice of stirring method causes a vortex, which drives water and semiconductor particle away from the centre of the reactor to the perimeter. Thus, photons from the top down will be incident on the centre of the reactor, where the concentration of the solution is low (Fig. 2.1).

In order to stir the semiconductor-electrolyte (e.g. photocatalyst-water) mixture, a magnetic stirrer was used to drive an inert PTFE magnetic stirring bar in the solution, as shown in Fig. 2.1. Conventional top down steel impeller blades would not be suitable for this application because of the risk of contamination of the blades with the semiconductor-electrolyte, i.e. through metallic leaching of nickel or chromium species. The nature of heterogeneous photocatalysis is such that the main interactions are that of the absorption of photons by the semiconductor, cleavage of water using charge carriers, and then release of product (H_2 , O_2 or both). In order for the photocatalyst to homogeneously absorb light (ignoring reflection), the photocatalyst particles must be mixed at a high enough radial velocity so that they do not sink to the bottom of the reactor, and maintain in constant motion close to the reactor walls. Having apparatus such as baffles would not benefit the absorption of light by the semiconductor since excessive mixing with water will not alter the reaction significantly. Water is later oxidised or reduced instantaneously, and gaseous product released as a dissolved gas in water. Therefore in this case, using a PTFE magnetic stirring bar to produce a radial

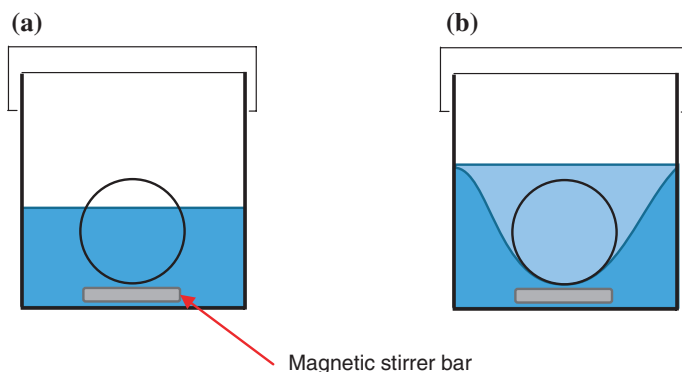


Fig. 2.1 Schematic of proposed reactor **a** without magnetic stirring, **b** with stirring

flow, and thus induce solid body rotation in the liquid—which is enough to form a temporary suspension—is more than satisfactory. More complex mixing is not necessary.

2.1.1 Reactor

A borosilicate cylindrical glass reactor was designed and then handmade by Labglass Ltd (4.5 cm radius, 11.5 cm height). The total volume was 730 cm³, including headspace (calculated by water displacement). The vessel is fitted with a flat high purity borosilicate side window, which is slightly bigger than the beam of the light source (40 mm Φ reactor window, 33 mm Φ beam). High purity borosilicate is suitable for a photocatalytic reactions as the low impurity content (such as iron) allows both UV and visible wavelengths of light to pass through without any absorption (Fig. 2.2).

The reactor was also fitted with two side ports (fitted with GL18 aperture caps and silicon septa) for purging and gas sampling. The top of the system was a PTFE screw thread aperture cap, with a detachable transparent borosilicate window. The reactor sealing mechanism was originally a 7 mm depth silicon ring which fitted between the glass and the top PTFE aperture cap. However, it was discovered that the sealing provided by the company was insufficient; the sealing would become dislodged during purging, and also during experiments. Despite numerous replacements from LabGlass, the sealing was a continuous problem and frequently disrupted and forced experiments to be stopped. Ultimately a solution was found whereby a very thin piece of silicon (0.5 mm, Altec Ltd) was cut to fit the reactor diameter. This method of sealing provided not only an airtight seal throughout the experiment, but also was able to withstand higher pressures generated when a high purging flow rate (in order to accelerate purge time).

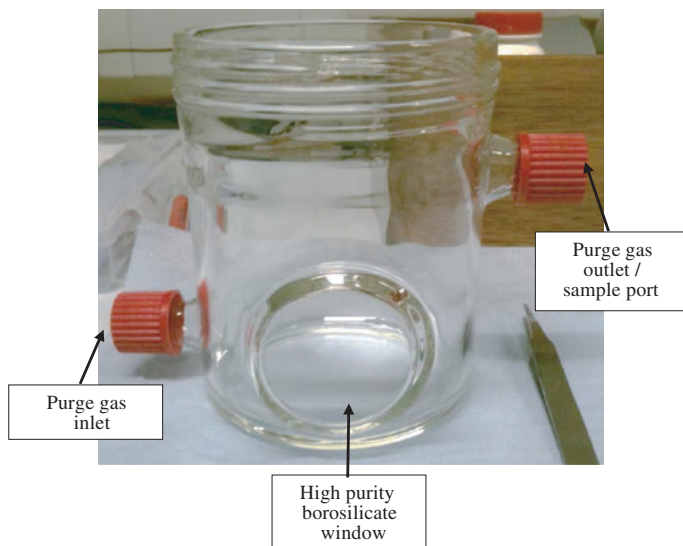


Fig. 2.2 Borosilicate reactor for water splitting batch reactions

2.1.2 Light Source

Two different xenon (Xe) lamps were purchased from Newport Spectra and TrusTech to act as artificial light sources. Xe lamps have a spectral profile akin to that of the solar spectrum, with intensity less than $20 \text{ mW m}^{-2} \text{ nm}^{-1}$ at $250 < \lambda < 800 \text{ nm}$ ¹⁵. A 300 W Xe lamp (TrusTech PLS-SXE 300/300UV) was used for oxygen, hydrogen, and water splitting, and also for calculating solar-to-hydrogen conversion efficiency. The higher power lamp source will in theory enable the probing of photocatalysts whose efficiencies are considerably small, as a larger photon flux will increase the rate of water splitting. A 150 W Xe lamp (Newport 6256 150 W Xe) was utilised for IQY measurements; the lower intensity of the 150 W Xe lamp prevented damage to the band pass filters, which absorb considerable amounts of light, up to 90 %.

The power from the lamp was calculated using a Silicon photodiode detector (190–1110 nm), with built in attenuator, connected to a handheld digital power meter (both purchased from Newport Spectra). Various long pass filters were used, from 400 to 550 nm, supplied by Comar Optics; enabling the selective use of either full arc or restricted visible light. Similarly, band pass filters were used in IQY measurements. These filters have a quoted centre wavelength, for example 400 nm, and the width of all pass-bands are 10 nm (395–405 nm).

2.2 Gas Chromatography: Selection and Calibration

2.2.1 Gas Chromatography Setup

A Varian 450 gas chromatograph (GC) was used to analyse the amounts of gaseous products from water splitting reactions (Fig. 2.3), and to monitor nitrogen levels within a batch reactor. Samples were taken by using a gas-tight syringe (Hamilton® 1000 μL). The GC was fitted with a TCD and molecular sieve 5A column, running with argon carrier gas (zero grade). As discussed in Sect. 1.2.2, argon is a suitable carrier gas for analysing concentrations of hydrogen, oxygen and nitrogen, due to the sufficiently low thermal conductivity—therefore all produced peaks will be positive, making integration easier during analysis (Table 2.1). Helium is an alternative, but is slightly more expensive, and would also yield negative peaks for oxygen and nitrogen due to the higher thermal conductivity, which would then be problematic during peak analysis. For these reasons it was not selected.

The signal from the GC's TCD produces a chromatogram on the Varian 450-GC software (an idealised version is shown in Fig. 2.4). The chromatograph is a plot of signal (μV) versus time (minutes); whereby the area under the signal

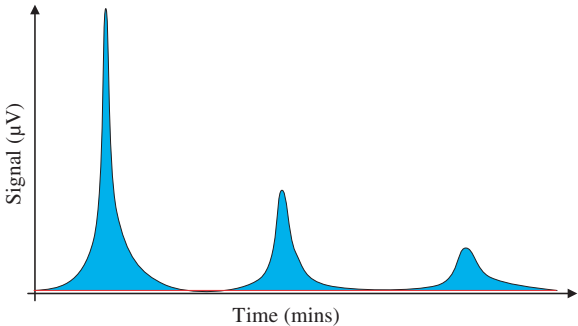
Fig. 2.3 Photograph of the gas chromatograph unit used during photocatalysis experiments



Table 2.1 Gases and corresponding thermal conductivity at STP [5]

Gas	Thermal conductivity (W m ⁻¹ K ⁻¹)
Hydrogen	0.1805
Helium	0.1513
Nitrogen	0.0259
Oxygen	0.0266
Argon	0.0177

Fig. 2.4 Idealised example chromatogram. A baseline is indicated by a horizontal *red* line, and integrated area under the curve (in $\mu\text{V min}$) is indicated by a shaded *blue* area



($\mu\text{V min}$) is proportional to the concentration of a specific gas, and each separate signal is separated in time, denoting different gases. By selecting an appropriate baseline, and performing an automatic integration via the software, an accurate signal area can be acquired.

In order to establish a reasonable signal, parameters were tuned to optimise peak separation, signal-to-noise ratio, and baseline fluctuations. Many water splitting experiments documented in the literature record gas concentrations at either 15 or 30 min intervals, with some elongated experiments recording every hour [3]. Therefore the total run time for each chromatogram should be less than 15 min, i.e. all necessary gases should appear in a 10 to 15 min window, or have a retention time (RT) less than 15 min. In gas chromatography, the parameters which governs RT of a gas are oven temperature, pressure and flow rate of carrier gas inside the column—two of which were consequently set to 50 °C, and 50 PSI to enable all gases (hydrogen, oxygen, nitrogen) to come through within a 10 min window. Signal-to-noise ratio and baseline fluctuations can be controlled by adjusting flow rate and TCD filament temperature. After optimisation, the most efficient flow rate was 10 cm³ min⁻¹ and 180 °C. In general, increasing the flow rate through the TCD decreased peak width, but dramatically decreased peak height/response. Therefore a low flow rate was chosen so that small concentrations of gases could be detected.

2.2.2 Standard Gas and Calibration

In order to correlate the response generated by the TCD on the GC to the actual gas composition, a calibration curve is used. By injecting known concentrations (and thus known molar amounts) of gas, and then monitoring the response, a graph of area (y) versus concentration (x) can be plotted. Then, by solving the equation of a line ($y = mx + c$), for any area, a concentration can be calculated.

To then acquire an accurate known concentration, a suitable standard gas was purchased from BOC. It comprises of 99 % zero grade argon, with appropriate amounts of H₂ (4000 ppm) and O₂ (2000 ppm), among other gases which might be produced as by-products in a half reaction in the presence of charge scavenger (1000 ppm CO, 1000 ppm CO₂ and 2000 ppm methane). By injecting different volumes of this gas into the GC, a calibration curve can be built (Fig. 2.5), along with a response factor (R). The R factor is calculated by plotting amount of gas versus area, then solving the equation of the straight line for where the line intercepts the x-axis. Generally the response factor (essentially an offset error) should be as close to zero as possible, implying a true linear relationship between gas amount and peak area. In reality however, this is not the case, due to errors in manual syringe sampling, TCD response and for oxygen error—a residual amount of air left in the syringe (dead volume). However, these can be corrected for simply using the R-factor in calculating the amount of gas being measured.

To establish a sampling error, 10 different samples of 0.5 cm³ standard gas was injected, and then average, standard deviation (SD, σ) and percentage error was calculated (Table 2.2). The percentage error was calculated by dividing the SD by the mean.

Using Table 2.2, it is possible to apply a percentage error on both future H₂ and O₂ sampling data, which can be applied to calibration curves (Fig. 2.5, Table 2.3).

According to the linear fit statistics, an unknown molar amount of hydrogen or oxygen can be calculated by knowing the area under the curve from a gas sample. For example an area of 86,000 $\mu\text{V min}$ is recorded by the GC for hydrogen. Using the equation of the line, $y = 55663x + 216.54$;

$$\left(\frac{86000 - 216.54}{55663} \right) = 1.54 \mu\text{mol of hydrogen} \quad (2.1)$$

The linear regression best fit line shows that for hydrogen calibration, $r^2 = 0.9994$, and for oxygen $r^2 = 0.9947$. These high values of r^2 also confirm that by knowing y, predicting x using $y = mx + c$ has a high degree of confidence/accuracy [6]. Essentially r-squared is a fraction which is used to determine how x changes linearly with y.

It is important to separate the oxygen measured from the standard gas, and that from air, which is left in the syringe tip (dead volume). From Table 2.2 it is evident that even a small amount of air in the syringe tip can influence the calibration,

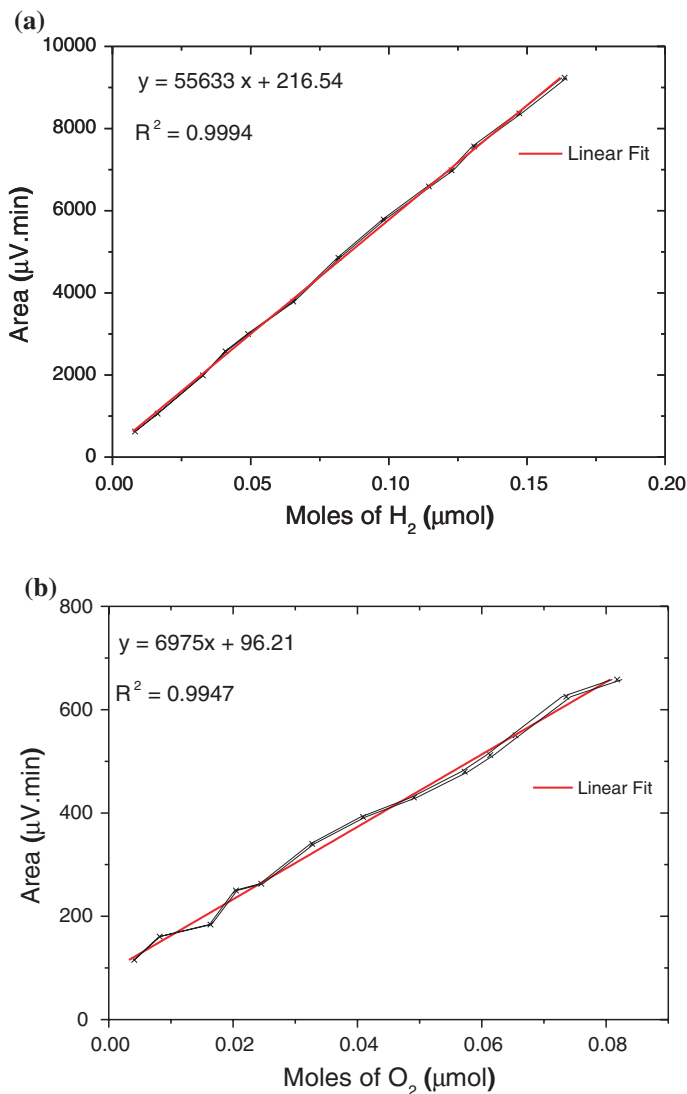


Fig. 2.5 GC area versus molar amount calibration curves for hydrogen (a), and oxygen (b). Equations of linear fits and R^2 values are noted in the *upper left* hand corner of the figure

increasing error—which is nearly double that of the standard error on a hydrogen sample, since no hydrogen exists freely in air. The air contaminant also comes from a small amount which is inside the injection port in the GC. All of which is taken into account for the calibration. The successful calibration of the GC means that gas amounts as low as 10^{-9} mol can be detected accurately.

Table 2.2 Area sampling data for H₂ and O₂ (0.5 cm³)

	Area (μV min)	
	H ₂	O ₂
	4896.1	390.5
	4834.4	394.5
	4831.0	389.2
	4885.1	388.2
	4876.7	399.5
	4867.5	397.6
	4845.9	391.1
	4849.8	393.3
	4888.6	393.9
	4820.3	399.0
Mean	4859.5	393.7
σ	25.4	3.8
% Error	0.52 %	0.97 %

SD was taken for entire population

2.3 General Characterisation

The following section details standard characterisation methods that are used for all necessary results sections, to avoid repetition.

2.3.1 UV-Vis Spectrophotometry

Absorption, reflection and transmission spectra were collected from a Shimadzu UV-2550 spectrophotometer fitted with an integrating sphere. The software provided (UV-Probe 2.33) enabled reflection to be directly converted to absorption by the Kubelka-Munk transformation. Typically, data would be collected from 250 to 800 nm, with an optimum slit width of 2 nm. This reduces noise whilst not compromising the accuracy of the data. The frequency of the data was 0.5 nm, as this was more than adequate enough to determine precise spectra.

2.3.2 PXRD

PXRD was performed on either a Rigaku RINT 2100 (40 kV, 40 mA, using a Cu source with $K_{a1} = 1.540562$ and $K_{a2} = 1.544398$) or a Bruker D4 (40 kV, 30 mA, using a Cu source with $K_{a1} = 1.54056$ and $K_{a2} = 1.54439$). A maximum 0.05° step size was used, at 5 s per step, covering a maximum range of 0–90° (2θ). Phase match and baseline corrections were performed on either MDI Jade, or

Table 2.3 Data table for Fig. 2.5

Hydrogen					
Syringe volume (cm ³)	Amount of H ₂ (cm ³)	Amount of H ₂ × 10 ⁻⁹ (m ³)	Moles of H ₂ × 10 ⁻⁸	Moles of H ₂ (μM)	Area (μV min)
0.05	0.0002	0.2	0.82	0.008	623.4
0.1	0.0004	0.4	1.64	0.016	1059.5
0.2	0.0008	0.8	3.27	0.033	1992.3
0.25	0.0010	1.0	4.09	0.041	2575.9
0.3	0.0012	1.2	4.91	0.049	3000.5
0.4	0.0016	1.6	6.54	0.065	3787.9
0.5	0.0020	2.0	8.18	0.082	4853.8
0.6	0.0024	2.4	9.82	0.098	5784.0
0.7	0.0028	2.8	11.50	0.115	6590.5
0.75	0.0030	3.0	12.30	0.123	6982.6
0.8	0.0032	3.2	13.10	0.131	7565.7
0.9	0.0036	3.6	14.70	0.147	8372.0
1	0.004	4.0	16.30	0.164	9237.7
Oxygen					
Syringe volume (cm ³)	Amount of O ₂ (cm ³)	Amount of O ₂ × 10 ⁻⁹ (m ³)	Moles of O ₂ × 10 ⁻⁸	Moles of O ₂ (μM)	Area (μV min)
0.05	0.0001	0.1	0.41	0.0041	115.5
0.1	0.0002	0.2	0.82	0.0082	160.7
0.2	0.0004	0.4	1.64	0.0164	184.1
0.25	0.0005	0.5	2.04	0.0204	250.0
0.3	0.0006	0.6	2.45	0.0245	263.1
0.4	0.0008	0.8	3.27	0.0327	340.0
0.5	0.0010	1.0	4.09	0.0409	392.4
0.6	0.0012	1.2	4.91	0.0491	430.0
0.7	0.0014	1.4	5.73	0.0573	480.1
0.75	0.0015	1.5	6.13	0.0613	512.0
0.8	0.0016	1.6	6.54	0.0654	550.3
0.9	0.0018	1.8	7.36	0.0736	625.1
1	0.0020	2.0	8.18	0.0818	658.4

Bruker's EVA software using the ICSD/JCPDS database. A powdered sample was flattened into an amorphous glass (Rigaku) or silicon (Bruker) well holder.

2.3.3 FE-SEM

A JEOL JSM-7401F was used for measuring particle size, examining agglomeration of particles and also performing EDX measurements. The main advantage of

using a Field Emission-SEM is that a greater resolution is possible (up to 6 times greater than conventional SEMs). Furthermore, electrostatic charging is greatly reduced on poorly conductive samples because lower acceleration voltages, without compromising image quality. Carbon tape was used as a conductive adhesive for the powdered samples.

2.3.4 TEM

Conventional TEM measurements were taken using a JEOL2010F, at an accelerating voltage of 200 keV. Powdered samples were diluted in chloroform, sonicated to disperse particle, and then dropwise added onto a conductive copper grid. Tilt studies and EDX measurements were also conducted on a JEOL2010F.

2.3.5 BET Specific Surface Area

Specific surface area was calculated via the BET method, using N₂ absorption by a Micromeritics TriStar 3000. Powdered samples were placed in a borosilicate vial, with a weight to surface area ratio of 1 g to 30 m² in order to acquire suitable data. Values of R² (linear regression) were tuned to be as close to 1 as possible, with all values ≥ 0.9998 .

2.3.6 ATR-FTIR Spectroscopy

ATR-FTIR spectroscopy was performed on a Perkin-Elmer 1605 FT-IR spectrometer in the wavenumber range from 400–4000 cm⁻¹ with a resolution of 0.5 cm⁻¹. Powdered samples were placed on the ATR crystal, and then compressed using a flat axial screw. Spectra were compared with literature examples, as there was available universal ‘search and match’ library for the instrument used.

2.3.7 Raman Spectroscopy

Raman spectroscopic measurements were performed on a Renishaw InVia Raman Microscope, using an Ar⁺ 514.5 nm excitation laser, and a wavenumber range from 100–2000 cm⁻¹. A ‘notch filter’ was used to cut out Rayleigh components, and a silicon standard was used for calibration at 520 cm⁻¹.

2.3.8 TGA-DSC-MS

Thermo Gravimetric Analysis-Differential Scanning Calorimetry-Mass Spectroscopy (TGA-DSC-MS) was performed on a Netzsch Jupiter TGA-DSC, connected to a Netzsch Aeolius MS, in an inert He atmosphere. The data was then processed using the Netzsch 'Proteus' thermal analysis software. Precursors (urea, thiourea) were placed in an alumina crucible, and calcined from 26.9 to 600 °C, over a period of 115 min. From the raw data, TGA data yields a plot of mass loss (%) versus temperature, DSC yields heat change (exothermic/endothermic reaction) versus temperature information, and MS monitors mass number (ion current, nA) relative concentration versus temperature.

2.3.9 Zeta Potential (ZP) Measurements

ZP measurements were performed using a Zetasizer nano ZS equipped with a He-Ne laser 633 nm, maximum 4mW power, and analysis was undertaken using the 'Zetasizer software'. Powdered samples were diluted in a 0.05 M aqueous NaCl solution, which acted as an electrolyte, increasing conductivity. A 5 cm³ sample was then sonicated for 30 min, and then placed into a ZP cuvette/cell with gold connectors. ZP was monitored as pH was changed from neutral (starting at ca. 7.7) to both alkaline and acidic conditions using NaOH and HCl respectively (manual titration). For each pH point, 5 measurements were taken, and the mean then calculated. The isoelectric point (IEP) is defined as the point of zero change at a set pH, and thus was recorded at ZP = 0.

2.3.10 XPS

XPS measurements were performed on a ThermoScientific XPS K-alpha surface analysis machine using an Al source. Analysis was performed on the Thermo Advantage software. After samples were placed under UHV, a sweep scan was performed from 100–4000 eV. Each sample was scanned 6 times at different points on the surface to eliminate point error and create an average. Specific elemental peaks were then identified, and analysed further.

2.3.11 Elemental Analysis

Elemental Analysis (EA) was performed on a Micro Elemental Analyzer (CE-400 CHN Analyser, Exeter Analytical Instruments). Accurate (± 0.1 %) weight percentages of carbon, nitrogen, hydrogen and trace elements were converted to atomic percentages before analysis.

References

1. Yi, Z., et al. (2010). An orthophosphate semiconductor with photooxidation properties under visible-light irradiation. *Nature Materials*, 9, 559–564.
2. Murphy, A. B., et al. (2006). Efficiency of solar water splitting using semiconductor electrodes. *International Journal of Hydrogen Energy*, 31, 1999–2017.
3. Chen, X., Shen, S., Guo, L., & Mao, S. S. (2010). Semiconductor-based photocatalytic hydrogen generation. *Chemical Reviews*, 110, 6503–6570.
4. Cabrera, M. I., Alfano, O. M., & Cassano, A. E. (1994). Novel Reactor for Photocatalytic Kinetic Studies. *Industrial and Engineering Chemistry Research*, 33, 3031–3042.
5. Tsederberg, N. V., & Cess, R. D. (1965). *Thermal conductivity of gases and liquids*. Cambridge, Massachusetts: MIT Press.
6. Seber, G. A. & Lee, A. J (2012). *Linear regression analysis* (Vol. 936). New York:Wiley.

Investigation into High Efficiency Visible Light
Photocatalysts for Water Reduction and Oxidation

Martin, D.J.

2015, XXVIII, 149 p. 76 illus., 62 illus. in color.,

Hardcover

ISBN: 978-3-319-18487-6